

**This is a self-archived version of an original article. This version may differ from the original in pagination and typographic details.**

**Author(s):** Hsu, Yi-Fang; Xu, Weiyong; Parviainen, Tiina; Hämäläinen, Jarmo A.

**Title:** Context-dependent minimisation of prediction errors involves temporal-frontal activation

**Year:** 2020

**Version:** Published version

**Copyright:** © 2019 the Author(s)

**Rights:** CC BY-NC-ND 4.0

**Rights url:** <https://creativecommons.org/licenses/by-nc-nd/4.0/>

**Please cite the original version:**

Hsu, Y.-F., Xu, W., Parviainen, T., & Hämäläinen, J. A. (2020). Context-dependent minimisation of prediction errors involves temporal-frontal activation. *NeuroImage*, 207, Article 116355.  
<https://doi.org/10.1016/j.neuroimage.2019.116355>



# Context-dependent minimisation of prediction errors involves temporal-frontal activation



Yi-Fang Hsu<sup>a,b,\*</sup>, Weiyong Xu<sup>c</sup>, Tiina Parviainen<sup>c</sup>, Jarmo A. Hämäläinen<sup>c</sup>

<sup>a</sup> Department of Educational Psychology and Counselling, National Taiwan Normal University, 10610, Taipei, Taiwan

<sup>b</sup> Institute for Research Excellence in Learning Sciences, National Taiwan Normal University, 10610, Taipei, Taiwan

<sup>c</sup> Jyväskylä Centre for Interdisciplinary Brain Research, Department of Psychology, University of Jyväskylä, 40014, Jyväskylä, Finland

## ARTICLE INFO

### Keywords:

Predictive coding  
Auditory perception  
Repetition suppression  
Repetition enhancement  
Magnetoencephalography (MEG)

## ABSTRACT

According to the predictive coding model of perception, the brain constantly generates predictions of the upcoming sensory inputs. Perception is realised through a hierarchical generative model which aims at minimising the discrepancy between predictions and the incoming sensory inputs (i.e., prediction errors). Notably, prediction errors are weighted depending on precision of prior information. However, it remains unclear whether and how the brain monitors prior precision when minimising prediction errors in different contexts. The current study used magnetoencephalography (MEG) to address this question. We presented participants with repetition of two non-predicted probes embedded in context of high and low precision, namely mispredicted and unpredicted probes. Non-parametric permutation statistics showed that the minimisation of precision-weighted prediction errors started to dissociate on early components of the auditory responses (including the P1m and N1m), indicating that the brain can differentiate between these scenarios at an early stage of the auditory processing stream. Permutation statistics conducted on the depth-weighted statistical parametric maps (dSPM) source solutions of the repetition difference waves between the two non-predicted probes further revealed a cluster extending from the frontal areas to the posterior temporal areas in the left hemisphere. Overall, the results suggested that context precision not only changes the weighting of prediction errors but also modulates the dynamics of how prediction errors are minimised upon the learning of statistical regularities (achieved by stimulus repetition), which likely involves differential activation at temporal-frontal regions.

## 1. Introduction

Our brain constantly generates predictions of the upcoming sensory inputs. The predictive coding model proposes that successful perception depends on minimising the discrepancy between predictions and the incoming sensory inputs (i.e., prediction errors) via feedback connections (Rao and Ballard, 1999; Friston, 2009; Summerfield et al., 2008; see Clark, 2013 for a review). Cortical responses can be understood as a transient expression of prediction errors (Friston, 2005; Feldman and Friston, 2010).

Notably, prediction errors are scaled depending on the precision (i.e., inverse variance) of the sensory inputs (Friston, 2005, 2009), which quantifies the degree of certainty about the variables (Feldman and Friston, 2010) and can be driven by internal factors such as attention as

well as external factors such as the statistical properties of sensory signals (Quiroga-Martinez et al., 2019). Specifically, in a reliable environment where contextual regularity is conspicuous, deviations eliciting prediction errors are weighted more to update predictions because they are informative. Conversely, in a volatile environment where contextual regularity is weak, deviations eliciting prediction errors are weighted less because they are rather imprecise (Clark, 2013; Schröger et al., 2015). Such precision-weighting mechanism would ensure that learning is primarily driven by reliable rather than volatile contexts. This idea was supported by neuroimaging studies showing that non-predicted tones embedded in temporally regular and random contexts are associated with different amounts of cortical activity. For example, electrocorticography (ECoG) research documented a significant difference on higher gamma activity when comparing deviant sounds presented in regular intervals

\* Corresponding author. Department of Educational Psychology and Counselling, National Taiwan Normal University, 162, Section 1, Heping E. Road, 10610, Taipei, Taiwan.

E-mail addresses: [yi-fang.hsu@cantab.net](mailto:yi-fang.hsu@cantab.net) (Y.-F. Hsu), [weiyong.w.xu@jyu.fi](mailto:weiyong.w.xu@jyu.fi) (W. Xu), [tiina.m.parviainen@jyu.fi](mailto:tiina.m.parviainen@jyu.fi) (T. Parviainen), [jarmo.a.hamalainen@jyu.fi](mailto:jarmo.a.hamalainen@jyu.fi) (J.A. Hämäläinen).

<https://doi.org/10.1016/j.neuroimage.2019.116355>

Received 11 March 2019; Received in revised form 16 October 2019; Accepted 11 November 2019

Available online 12 November 2019

1053-8119/© 2019 The Authors. Published by Elsevier Inc. This is an open access article under the CC BY-NC-ND license (<http://creativecommons.org/licenses/by-nc-nd/4.0/>).

and random intervals (Dürschmid et al., 2016). Importantly, it is not only temporal precision but also spectral precision that can modulate the gain of prediction errors. Manipulation of spectral precision is commonly adopted to reveal the neurophysiological underpinnings of the prediction of “what” happens in the sensory environment (Lange, 2009; Hsu et al., 2013; Barascud et al., 2016; Southwell et al., 2017; Auksztulewicz et al., 2018). Using the oddball paradigm to elicit mismatch negativity (MMN), electroencephalography (EEG) research reported a significant difference on the event-related potentials (ERPs) when comparing deviant sounds embedded in a standard sequence and an equiprobable sequence (Jacobsen and Schröger, 2001; see Näätänen et al., 2005 for a review). The dissociation was also found in the earlier time window such as the N1, which is an electrophysiological indicator for automatic predictive processing (Schafer and Marcus, 1973; Schafer et al., 1981; Lange, 2009; SanMiguel et al., 2013; Timm et al., 2013; Hsu et al., 2014a, 2014b, 2016; see Bendixen et al., 2012 for a review). When compared with predicted sounds, non-predicted sounds embedded in a spectrally regular stream (referred to as mispredicted sounds) are associated with enhanced N1, while non-predicted sounds embedded in a spectrally random stream (referred to as unpredicted sounds) are associated with suppressed N1 (Hsu et al., 2015, 2018). These findings highlighted the necessity to distinguish between prediction errors triggered by a precise spectral prediction that is not fulfilled and prediction errors triggered by an imprecise spectral prediction.

A recent magnetoencephalography (MEG) research further investigated the cortical dynamic of the minimisation of prediction errors in contexts of different precision (Hsu et al., 2019). Minimisation of prediction errors was achieved by stimulus repetition, which is known to result in the extraction of statistical regularities to optimise predictions (i.e., to minimise prediction errors) (Summerfield et al., 2008, 2011). Meanwhile, precision was manipulated via changes in the familiarity of prime tones. Participants listened to repetition of probe tones preceded by familiar prime tones (which elicited prediction errors in a high precision context; referred to as mispredicted condition) and probe tones preceded by unfamiliar prime tones (which elicited prediction errors in a low precision context; referred to as unpredicted condition). It was found that the minimisation of prediction errors was modulated by precision on N2m but not N1m. The absence of dissociation on the N1m came as a surprise. One possible explanation is that the N1m merely reflects the overall reduction of prediction errors regardless of precision weighting; the minimisation of prediction errors only differentiates as a function of precision later in the auditory processing stream. An alternative hypothesis is that the N1m is an expression of precision-weighted prediction errors. The lack of evidence was due to the manipulation of precision (via changes in the familiarity of prime tones) being too subtle for listeners to detect automatically.

To investigate whether the brain can differentially minimise

prediction errors as a function of precision at an early stage of the auditory processing stream, here we adopted a more pronounced manipulation of precision in an MEG experiment. Minimisation of prediction errors was operationalised via stimulus repetition as in our previous research. Meanwhile, in order to augment the contrast between mispredicted and unpredicted conditions, precision was manipulated via changes in the orderliness of prime tones based on the experimental design in Hsu et al. (2015), given that stimulus regularity was reported to robustly modulate the neural signatures of predictive (un)certainly (Barascud et al., 2016; Southwell et al., 2017; Auksztulewicz et al., 2018). Specifically, we presented participants with repetition of tone quintets (which consisted of four prime tones and one probe tone). In most cases, a probe tone followed the ascending pattern of primes tones (referred to as predicted condition in Fig. 1A top), which served as a baseline here. Crucially, there were two oddball scenarios when a probe tone was considered non-predicted: a probe tone violating the ascending pattern of prime tones when the listener was more certain of what the next stimulus could be (which triggered prediction errors in a high precision context; referred to as mispredicted condition in Fig. 1A middle) and a probe tone nested in prime tones of no existing pattern when the listener was less certain of the prediction he/she is making (which triggered prediction errors in a low precision context; referred to as unpredicted condition in Fig. 1A bottom). To maintain participants' attention on the stimuli (which can interact with the prediction mechanism otherwise), we required participants to press a key as soon as they detected a softer tone as a cover task. If the minimisation of prediction errors is modulated by precision, there should be a repetition (1st/2nd presentations)  $\times$  context (predicted/mispredicted/unpredicted probes) interaction. In particular, the repetition effect of mispredicted and unpredicted probes should differ from each other.

## 2. Materials and methods

### 2.1. Participants

23 healthy adults (average age 23; 6 males; 21 right-handed) with no history of neurological, psychiatric, or visual/hearing impairments as indicated by self-report participated in the experiment. Participants gave written informed consent and were paid for participation. Ethical approval was granted by the research ethics committee at National Taiwan Normal University. 2 participants were excluded from data analysis for excessive measurement noise, leaving 21 participants in the final sample (average age 23; 6 males; 19 right-handed).

### 2.2. Stimuli

14 sinusoidal tones were generated using Sound Forge Pro 10.0 (Sony

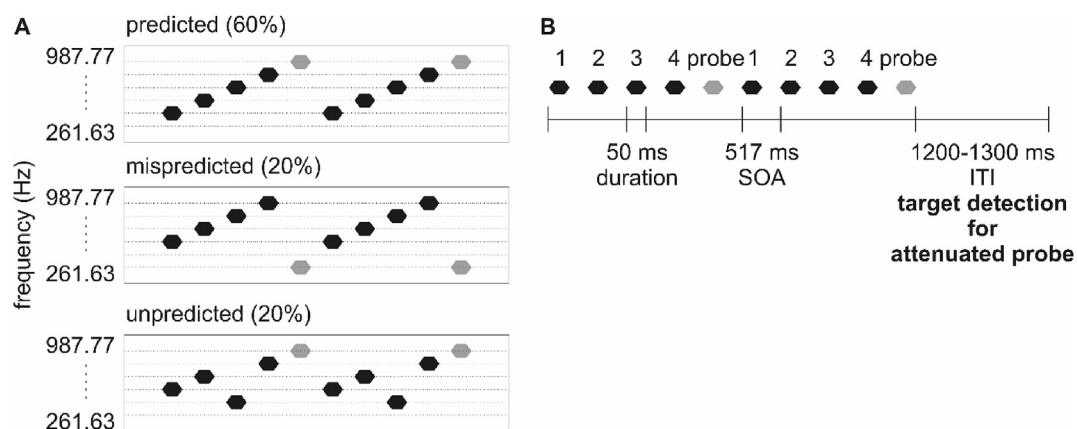


Fig. 1. Stimulus and paradigm. A. Repetition of tone quintet in the predicted (top), mispredicted (middle), and unpredicted (bottom) conditions. B. Time course of a trial.

Creative Software Inc.). The duration of each tone was 50 ms (including 5 ms rise/fall times). The frequency of each tone was within the range of 261.626–987.767 Hz, matching the absolute frequency of a series of 14 natural keys on a modern piano (i.e., C4 D4 E4 F4 G4 A4 B4 C5 D5 E5 F5 G5 A5 B5) (Table 1).

From the pool of 14 tones, a total of 500 tone quintets (consisting of four prime tones and one probe tone) were created. In the predicted condition, which comprised 300 tone quintets, the frequency of the four prime tones was ascending in steps of one natural key and the frequency of the probe tone was one natural key higher than the fourth prime tone in the series (e.g., E4-F4-G4-A4-B4). Here, the probe tone followed the ascending pattern (Fig. 1A top). In the mispredicted condition, which comprised 100 tone quintets, the frequency of the four prime tones was ascending in steps of one natural key and the frequency of the probe tone was two natural keys lower than the first prime tone in the series (e.g., E4-F4-G4-A4-C4). Here, the probe tone broke the ascending pattern (Fig. 1A middle). In the unpredicted condition, which comprised 100 tone quintets, the frequency of each tone was determined by random sampling without replacement, with the exception of any continuously rising or falling sequence to avoid the step inertia expectation (e.g., E4-C4-G4-A4-F4). Here, the probe tone cannot be predicted because there was no existing pattern (Fig. 1A bottom).

### 2.3. Procedures

A total of 5 blocks of 100 trials were presented. A grey fixation cross against black background remained on the screen for the duration of each block (viewed from a distance of 120 cm). In each trial, a tone quintet was presented twice and each tone was separated by a 517 ms stimulus onset asynchrony (SOA). The tones were presented with an intensity of maximum 70 dB (measured in dBC; range 60–70 dB). In each condition, 10 percent of the probe tones in their 2nd presentation were of attenuated loudness by 20 dB to serve as targets for the cover task. To maintain participants' attention on the stimuli, we required participants to press a key as soon as they detected a softer tone (without being informed that targets would only appear at the position of the probe tones in their 2nd presentation). Each trial was followed by a jittered inter-trial interval (ITI) of 1200–1300 ms (Fig. 1B). The whole experiment took around 50 min (i.e., 500 trials x 5970 ms). Presentation (Neurobehavioral Systems, Inc., USA) was used for stimulus presentation. Stimulation was randomised individually for each participant and delivered through a panel speaker situated in front of the participant.

### 2.4. Data recording and analysis

MEG data was collected using a 306 channel whole-head device (Elekta Neuromag, Finland) in a magnetically shielded room at National Taiwan University. The sampling rate was 1000 Hz. A high-pass filter of 0.1 Hz was used. Continuous head position monitoring was used based on four Head-Position Indicator (HPI) coils, with two at the forehead and two behind the ears. Electro-oculography (EOG) was recorded using electrodes lateral to each eye and above and below the right eye.

Offline, head movements were corrected and external noise sources were attenuated using the temporal extension of the source subspace separation algorithm (Taulu et al., 2005) in the MaxFilter program (Elekta Neuromag, Finland).

After the initial head movement correction, the data was analysed

using MNE-Python (0.15) (Gramfort et al., 2013). The MEG signal was resampled at 250 Hz and filtered at 1–40 Hz using a bandpass overlap-add FIR filter (filter direction: zero-phase; transition bandwidth: 1 Hz for high-pass and 10 Hz for low-pass). Then independent component analysis (ICA) using fastICA algorithm (Hyvärinen and Oja, 2000) was applied to remove eye blinks, horizontal eye movements, and cardiac artifacts. Epochs extended from –200 ms to 500 ms relative to the onset of the probe using a 200 ms pre-stimulus baseline. We rejected segments time-locked to targets, segments where a key press occurred for the cover task, and segments with over 4000 fT/cm peak-to-peak values in gradiometers or 4000 fT peak-to-peak values in magnetometers. In order to avoid the confound of difference in signal-to-noise ratio between conditions, trial numbers were equalized to the lowest number across all conditions using the MNE-python function 'equalize\_epoch\_counts' resulting in approximately 80–90 trials per condition for each participant.

In order to determine the P1m, the N1m, and the late time windows, we first identified the peak of P1m and N1m from the sensor-level grand averages of all conditions across sensors, and then defined the P1m time window as  $\pm 20$  ms around the peak at 64 ms (i.e., 44–84 ms) and N1m time window as  $\pm 30$  ms around the peak at 118 ms (i.e., 88–148 ms). The late time window (i.e., 152–500 ms) was picked for a more exploratory purpose. In other words, the time windows were selected based on the peak of the respective response independent of conditions. Hereafter, all permutation statistics were performed in time resolved manner separately for the P1m, the N1m, and the late time windows. In order to examine the repetition (1st/2nd presentations) x context (predicted/mispredicted/unpredicted probes) interaction, which would indicate whether the minimisation of prediction errors (manipulated via stimulus repetition) is modulated by precision (manipulated via changes in the orderliness of prime tones), we calculated the difference waves between repeated presentations (i.e., 1st - 2nd presentation) for each context level as inputs for all permutation statistics.

Sensor-level statistical comparisons were carried out using non-parametric permutation statistics with spatial and temporal clustering. The repetition difference waves were exported to BESA Statistics 2.0 for permutation statistics based on ANOVA with three context levels. The analyses were performed on the combined gradiometers (i.e., vector sum of the two gradiometers) because gradiometers are less sensitive to noise than magnetometers. Cluster alpha level was 0.05 and number of permutations was 1000.

Source-level statistical comparisons were carried out in MNE-Python to further examine the origins of effects found in the sensor-level analysis. The MEG data was co-registered to the fsaverage MRI template with three parameter scaling. A boundary element model of the inner skull created from the fsaverage MRI template was used because no individual MRIs were available. The covariance matrix for the depth-weighted statistical parametric maps (dSPM) of the minimum-norm source solutions used the pre-stimulus baseline from the individual epoch. Depth weighting of 0.8 was used with loose dipole orientations. Permutation statistics with spatial and temporal clustering were based on t-tests (MNE-python function 'spatio\_temporal\_cluster\_1samp\_test') on the repetition difference waves for pairs of context levels. The contrasts between mispredicted and unpredicted probes, mispredicted and predicted probes, as well as unpredicted and predicted probes were conducted separately. Cluster alpha level was 0.05 and number of permutations was 1000.

**Table 1**

Frequency of each tone.

|                | C4     | D4     | E4     | F4     | G4     | A4     | B4     |
|----------------|--------|--------|--------|--------|--------|--------|--------|
| Frequency (Hz) | 261.63 | 293.67 | 329.63 | 349.23 | 392.00 | 440.00 | 493.88 |
|                | C5     | D5     | E5     | F5     | G5     | A5     | B5     |
| Frequency (Hz) | 523.25 | 587.33 | 659.26 | 698.46 | 783.99 | 880.00 | 987.77 |

### 3. Results

Fig. 2 shows the sensor-level grand averages of the predicted, mispredicted, and unpredicted conditions over representative left and right temporal channels.

#### 3.1. P1m time window (44–84 ms)

##### 3.1.1. Sensor-level analysis

Permutation statistics in the P1m time window showed a main effect of context for the repetition difference waves, indicating a significant repetition  $\times$  context interaction ( $p = 0.005$ , cluster time points 44–84 ms). Post hoc pairwise ANOVA between three context levels further showed that the repetition difference waves differed between mispredicted and unpredicted probes ( $p = 0.005$ , cluster time points 44–84 ms) with the spatial clustering of the channels suggesting a right lateralization of the effect. Meanwhile, the repetition difference waves differed between mispredicted and predicted probes ( $p = 0.017$ , cluster time points 44–84 ms) with the spatial clustering of the channels suggesting a right lateralization of the effect but not between unpredicted and predicted probes (Fig. 3A left).

To further examine the direction of repetition effect in each context level, permutation statistics based on t-tests were performed as post hoc analyses. Significant repetition effect was found in predicted probes (repetition enhancement in 2 clusters:  $p = 0.005$ , cluster time points 44–84 ms and  $p = 0.036$ , cluster time points 44–64 ms) and mispredicted probes (repetition enhancement:  $p < 0.001$ , cluster time points 44–84 ms) but not in unpredicted probes (Fig. 3A right).

#### 3.1.2. Source-level analysis

The source-level analysis failed to find statistically significant effect between mispredicted and unpredicted probes. However, the rest of the findings converged with the sensor-level results. There was a statistically significant effect between the mispredicted and predicted probes with the cluster having two foci, one in the Sylvian fissure and the other in the posterior temporo-parietal area in the right hemisphere but not between unpredicted and predicted probes (Fig. 3A lower).

#### 3.2. N1m time window (88–148 ms)

##### 3.2.1. Sensor-level analysis

Permutation statistics in the N1m time window showed a main effect of context for the repetition difference waves, indicating a significant repetition  $\times$  context interaction ( $p = 0.002$ , cluster time points 96–148 ms). Post hoc pairwise ANOVA between three context levels further showed that the repetition difference waves differed between mispredicted and unpredicted probes ( $p = 0.005$ , cluster time points 100–148 ms) with the spatial clustering of the channels suggesting a left lateralization of the effect. Meanwhile, the repetition difference waves differed between mispredicted and predicted probes ( $p < 0.001$ , cluster time points 96–148 ms) with the spatial clustering of the channels suggesting a left lateralization of the effect but not between unpredicted and predicted probes (Fig. 3B left).

To further examine the direction of repetition effect in each context level, permutation statistics based on t-tests were performed as post hoc analyses. Significant repetition effect was found in predicted probes (repetition enhancement:  $p < 0.001$ , cluster time points 104–144 ms)

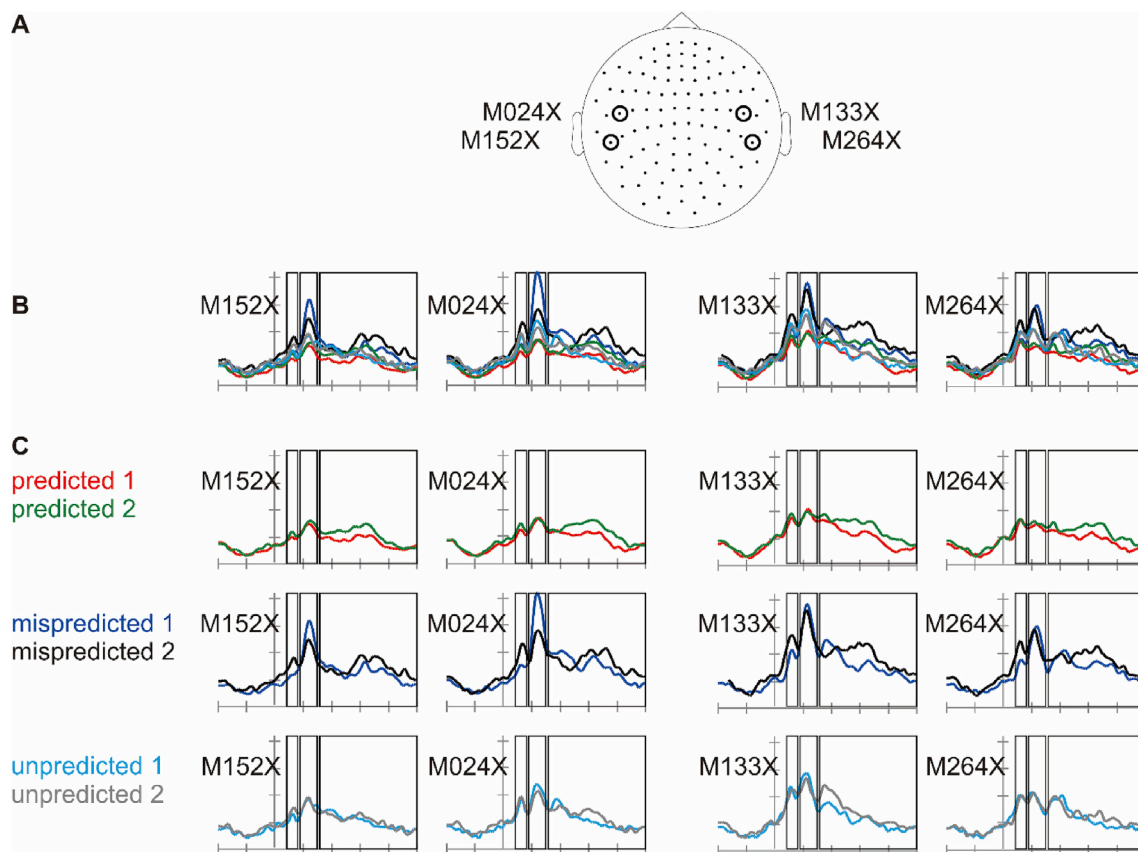
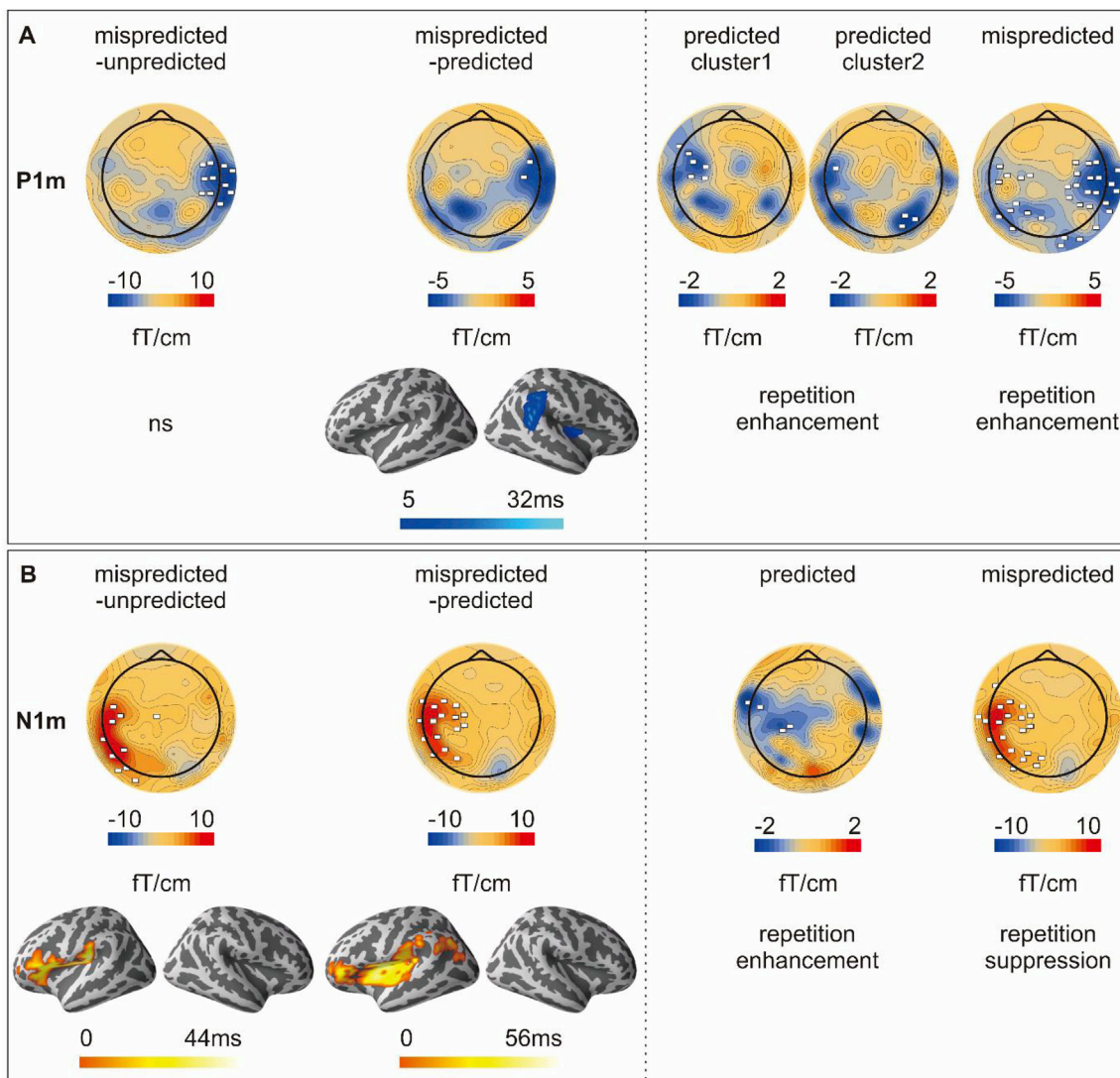


Fig. 2. A. Channel location schematics. The circles mark the representative left (M152X, M024X) and right (M264X, M133X) temporal channels. The notation X is used to indicate the vector sums of the two orthogonal gradiometers at each channel location (e.g., M152X represents the vector sums of left temporal channels M1521 and M1522, M264X represents the vector sums of right temporal channels M2641 and M2642). B and C. Sensor-level grand averages of the predicted, mispredicted, and unpredicted conditions over representative left and right temporal channels, displayed as overlaid (in B) and separated (in C). Vertical lines mark the onset of the probe. The three transparent boxes respectively mark the P1m (44–84 ms), the N1m (88–148 ms), and the late time windows (152–500 ms). Vertical scale is 10 fT/cm per mark. Horizontal scale is 100 ms per mark.



**Fig. 3.** Cluster-based permutation statistics in the P1m (A) and N1m (B) time windows. **Left** side of the dotted line shows the repetition effects between context levels. **Right** side of the dotted line shows the repetition effects within context levels (as post hoc observations). The rectangles in the topographies mark the gradiometers forming the significant cluster. The colour scale in the topographies indicates the magnetic field gradient strength (fT/cm). The colour scale in the source plots indicates the duration of the cluster in time (ms) and the direction of the effect (cold colours signify negative source strength and warm colours signify positive source strength).

and mispredicted probes (repetition suppression:  $p < 0.001$ , cluster time points 96–148 ms) but not in unpredicted probes (Fig. 3B right).

### 3.2.2. Source-level analysis

The source-level results converged with the sensor-level results, showing a statistically significant effect between mispredicted and unpredicted probes. Specifically, we found a cluster extending from the frontal areas to the posterior temporal areas in the left hemisphere. Similar to the sensor-level results, there was a statistically significant effect between the mispredicted and predicted probes with a cluster extending from the frontal areas to the posterior temporal areas in the left hemisphere but not between unpredicted and predicted probes (Fig. 3B lower).

### 3.3. Late time window (152–500 ms)

Permutation statistics in the later time window did not show any significant effect. Therefore, further statistical analysis was not performed.

### 3.4. Additional analysis on tone frequency effect

The current study maintained a fixed frequency range from which the tone quintets were constructed (261.626–987.767 Hz), which led to an inevitable imbalance in the average frequency of tones between conditions here (i.e., predicted > unpredicted > mispredicted). In order to exclude the possibility that the reported effects of interest were due to tone frequency effect, we contrasted neuronal responses to tones of highest and lowest frequencies via sensor-level statistical comparisons using non-parametric permutation statistics with spatial and temporal clustering. There were significant differences between the two tones (P1m:  $p < 0.001$ , cluster time points 44–84 ms; N1m:  $p < 0.001$ , cluster time points 88–136 ms), with maximal difference over the bilateral temporal areas at the end of the P1m time window and from the beginning of the N1m time window. Specifically, neuronal responses were larger to tones of highest than lowest frequencies. The pattern was opposite to what was found in the P1m and N1m time windows, where mispredicted condition (where the average frequency was the lowest) elicited the largest neuronal responses (Fig. 2C). Therefore, the observed

differences between conditions cannot be attributed to tone frequency effect.

#### 4. Discussion

The current study used MEG to examine the neuronal underpinnings of the minimisation of prediction errors in context of different precision. The minimisation of prediction errors was operationalised via stimulus repetition. Meanwhile, precision was manipulated via changes in the orderliness of prime tones based on the experimental design in Hsu et al. (2015), given that stimulus regularity was reported to robustly modulate the neural signatures of predictive (un)certainly (Barascud et al., 2016; Southwell et al., 2017; Auksztulewicz et al., 2018). Specifically, we presented participants with repetition of predicted probes and two non-predicted probes embedded in context of high and low precision, namely mispredicted and unpredicted probes. While mispredicted probes came after four primes arranged in ascending pattern, unpredicted probes came after four primes determined by pseudorandom sampling where there was no existing pattern.

We reported the novel finding that the minimisation of precision-weighted prediction errors started to dissociate on early components of the auditory responses. In the P1m time window, the minimisation of mispredicted and unpredicted errors diverged over right temporal regions. This was due to the fact that repetition of mispredicted probes elicited neuronal enhancement (mainly over right temporal regions) whereas repetition of unpredicted probes did not modulate neuronal responses. In the N1m time window, the minimisation of mispredicted and unpredicted errors diverged over left temporal regions. This was due to the fact that repetition of mispredicted probes elicited neuronal suppression (mainly over left temporal regions) whereas repetition of unpredicted probes did not modulate neuronal responses. The dissociation was further supported by the findings that the repetition difference waves differed between mispredicted and predicted probes but not between unpredicted and predicted probes in both P1m and N1m time windows. Notably, the current study is different from previous research reporting the brain's capacity to model the auditory context in the MMN (e.g., Schröger and Wolff, 1996; Bendixen et al., 2008), which is by default a difference wave. Meanwhile, while the MMN literature nicely explored the distinction between deviant sounds embedded in a standard sequence and an equiprobable sequence (Jacobsen and Schröger, 2001; see Näätänen et al., 2005 for a review), which resembled our manipulation of context precision, there was little attempt to track how such dissociation might develop as listeners learn to extract new structures in the auditory environment through stimulus repetition. In contrast, the current study was designed to look into this issue. Importantly, our results extend the notion in the predictive coding model of perception that context precision can adjust the weighting of prediction errors (Friston, 2005, 2009; Feldman and Friston, 2010; Schröger et al., 2015; Hsu et al., 2015, 2018). Specifically, we demonstrated that context precision can also influence the dynamics of how prediction errors are minimised upon the learning of statistical regularities (achieved by stimulus repetition), as the minimisation of mispredicted and unpredicted errors seems to recruit distinct networks.

In general, the earliest component that is consistently modulated by the prediction mechanism in adults is the N1m. Here we demonstrated a previously unreported earlier modulation of context precision on the P1m. P1m (and its electrical counterpart P1) is considered an obligatory component of auditory response. Its amplitude was reported to substantially suppress when paired stimuli were presented (Waldo and Freedman, 1986; Dolu et al., 2001). This was thought to reflect the mechanism of sensory gating, which filters out redundant information to prevent overloading the limited capacities of higher-order stages in auditory processing. While the main generators of P1m were localised at the lateral portion of Heschl's gyrus (ECoG: Liegeois-Chauvel et al., 1994; MEG: Pelizzone et al., 1987; Reite et al., 1988; Makela et al., 1994; Edgar et al., 2003; see Eggermont and Ponton, 2002 for a review), the major

source contributing to the sensory gating was localised at the frontal lobes (ECoG: Korzyukov et al., 2007; EEG: Knott et al., 2009; Weisser et al., 2001), suggesting that temporal-frontal interaction is required to work in concert to produce sensory gating (Grunwald et al., 2003). Intriguingly, our finding is in contrast with the literature on sensory gating. Specifically, repetition of mispredicted probes elicited P1m enhancement mainly over right temporal regions, whereas repetition of unpredicted probes failed to elicit significant effect. One mechanism underlying the presence and absence of repetition enhancement (rather than repetition suppression) for mispredicted and unpredicted probes might be related to auditory trace formation. It was reported that P1m increased with the number of standard stimulus repetition in the oddball paradigm (i.e., repetition positivity: Haenschel et al., 2005; Baldeweg, 2007), which likely represents sensory memory formation in the auditory cortex. It is possible that auditory trace formation is more efficient in high than low precision context. Another candidate mechanism is attention. Although P1m was long considered a preattentive component in information processing, there was evidence that selective attention could enhance the P1m (Giuliano et al., 2014). Therefore, it might be that repetition of mispredicted probes attracted more attention than repetition of unpredicted probes. This would mean to say that more attention is allocated to the processing of prediction errors embedded in high than low precision context.

On the other hand, N1m is thought to represent a distinct aspect of auditory information processing. The sources of the N1m are shown in the auditory cortices near planum temporale (Picton et al., 2000; Ponton et al., 2002), which is close to sources of the P1m (Yvert et al., 2005). It is believed that N1m (and its electrical counterpart N1) reflects multiple processes of signalling changes in the auditory environment (Näätänen and Picton, 1987; Crowley and Colrain, 2004). Previous research on the N1m refractory properties already documented that repeated stimuli led to suppressed activity (Näätänen and Picton, 1987; Budd et al., 1998; Jääskeläinen et al., 2004; Grau et al., 2007; Boutros et al., 2011; Recasens et al., 2015). Mounting evidence further supports the idea that N1m indicates the operation of an internal predictive mechanism, as expected stimuli also led to suppressed activity, possibly signalling the reduced prediction errors (Schafer and Marcus, 1973; Schafer et al., 1981; Lange, 2009; Todorovic et al., 2011; Todorovic and de Lange, 2012; SanMiguel et al., 2013; Timm et al., 2013; Hsu et al., 2014a, 2014b, 2016). Here we found that repetition of mispredicted probes elicited N1m suppression mainly over left temporal regions, whereas repetition of unpredicted probes failed to elicit significant effect. The mispredicted-unpredicted dissociation provides further evidence that the minimisation of prediction errors is context-dependent.

The results of sensor-level analyses were confirmed and extended in source-level analyses. Permutation statistics conducted on the dSPM source solutions of the repetition difference waves indicated that the context-dependent minimisation of prediction errors involves temporal-frontal activation. Specifically, in the N1m time window, contrast between mispredicted and unpredicted probes revealed a cluster extending from the frontal areas to the posterior temporal areas in the left hemisphere. However, the mispredicted versus unpredicted contrast at the P1m time window was significant at the sensor-level but not at the source-level. This could be due to the sensor-level analyses using information only from the combined gradiometers while the source reconstruction was based on both gradiometers and magnetometers. Further, the amount of spatial information feeding into the clustering was much larger for the source-level analyses which might increase the likelihood of a null finding.

Interestingly, the repetition of predicted probes (which served as a baseline condition) was associated with enhancement of P1m and N1m (at left temporal region). At first glance, it seems contradictory to a large body of literature concerning repetition suppression on early components of the auditory responses (P1m: Waldo and Freedman, 1986; Dolu et al., 2001; N1m: Näätänen and Picton, 1987; Budd et al., 1998; Jääskeläinen et al., 2004; Grau et al., 2007; Boutros et al., 2011; Recasens et al., 2015).

However, given that predicted probes were the fifth tones following the ascending pattern in each trial here, it is not really surprising that there was little prediction error to begin with (i.e., floor effect). Meanwhile, it was reported that recurrent presentation of predicted tones could trigger enhanced auditory responses (P1/P1m: Haenschel et al., 2005; Baldeweg, 2007; N1/N1m: Hsu et al., 2016), which might be due to sparser stimulus representation (Desimone, 1996; Wiggs & Martin, 1998), escalating learning function (Karhu et al., 1997), and heightened global expectation. The floor effect combined with one or more of these factors might account for our finding of enhanced P1m and N1m for the repetition of predicted probes. It is noteworthy that repetition enhancement is also a well-documented phenomenon in functional magnetic resonance imaging (fMRI) studies (Henson et al., 2000; Fiebach et al., 2005; Gagnepain et al., 2008; Soldan et al., 2008; Müller et al., 2013; Subramaniam et al., 2012), which might be related to stimulus recognition, network formation, and memory retrieval (see Segaert et al., 2013 for a review).

Overall, the current study shows that the minimisation of precision-weighted prediction errors can be dissociated at relatively early stage of the auditory processing stream. Context precision not only changes the weighting of prediction errors but also modulates the dynamics of how prediction errors are minimised upon the learning of statistical regularities (achieved by stimulus repetition), which likely involves differential activation at temporal-frontal regions.

### Author contributions

Y-FH and JAH designed and performed research. Y-FH, WX, and JAH analysed data; Y-FH, TP, and JAH wrote the paper.

### Declaration of competing interest

The authors declare no competing financial interests.

### Acknowledgement

This work was supported by Taiwan Ministry of Science and Technology (grant number MOST105-2410-H-003-145-MY3 and MOST107-2636-H-003-001) to YFH. We thank Imaging Center for Integrated Body, Mind, and Culture Research at National Taiwan University (funded by Taiwan Ministry of Science and Technology) for technical and facility supports. We also thank Miss YC Chung, Mr HE Lo, and Mr HS Huang for assistance with MEG data collection.

### References

- Aukszulewicz, R., Schwiedrzik, C.M., Thesen, T., Doyle, W., Devinsky, O., Nobre, A.C., Schroeder, C.E., Friston, K.J., Melloni, L., 2018. Not all predictions are equal: "what" and "when" predictions modulate activity in auditory cortex through different mechanisms. *J. Neurosci.* 38 (40), 8680–8693.
- Baldeweg, T., 2007. ERP repetition effects and mismatch negativity generation: a predictive coding perspective. *J. Psychophysiol.* 21 (3–4), 204–213.
- Barascud, N., Pearce, M.T., Griffiths, T.D., Friston, K.J., Chait, M., 2016. Brain responses in humans reveal ideal observer-like sensitivity to complex acoustic patterns. *Proc. Natl. Acad. Sci.* 113 (5), E616–E625.
- Bendixen, A., Prinz, W., Horváth, J., Trujillo-Barreto, N.J., Schröger, E., 2008. Rapid extraction of auditory feature contingencies. *Neuroimage* 41 (3), 1111–1119.
- Bendixen, A., SanMiguel, I., Schröger, E., 2012. Early electrophysiological indicators for predictive processing in audition: a review. *Int. J. Psychophysiol.* 83, 120–131.
- Boutros, N.N., Gjini, K., Urbach, H., Pflieger, M.E., 2011. Mapping repetition suppression of the N100 evoked response to the human cerebral cortex. *Biol. Psychiatry* 69, 883–889.
- Budd, T.W., Barry, R.J., Gordon, E., Rennie, C., Michie, P.T., 1998. Decrement of the N1 auditory event-related potential with stimulus repetition: habituation vs. refractoriness. *Int. J. Psychophysiol.* 31 (1), 51–68.
- Clark, A., 2013. Whatever next? Predictive brains, situated agents, and the future of cognitive science. *Behav. Brain Sci.* 36, 181–204.
- Crowley, K.E., Colrain, I.M., 2004. A review of the evidence for P2 being an independent component process: age, sleep and modality. *Clin. Neurophysiol.* 115, 732–744.
- Desimone, R., 1996. Neural mechanisms for visual memory and their role in attention. *Proc. Natl. Acad. Sci.* 93 (24), 13494–13499.
- Dolu, N., Suer, C., Ozesmi, C., 2001. A comparison of the different interpair intervals in the conditioning-testing P50 paradigms. *Int. J. Psychophysiol.* 41, 265–270.
- Dürschmid, S., Edwards, E., Reichert, C., Dewar, C., Hinrichs, H., Heinze, H.J., Knight, R.T., 2016. Hierarchy of prediction errors for auditory events in human temporal and frontal cortex. *Proc. Natl. Acad. Sci.* 113 (24), 6755–6760.
- Edgar, J.C., Huang, M.X., Weisend, M.P., Sherwood, A., Miller, G.A., Adler, L.E., Canive, J.M., 2003. Interpreting abnormality: an EEG and MEG study of P50 and the auditory paired-stimulus paradigm. *Biol. Psychol.* 65, 1–20.
- Eggermont, J.J., Ponton, C.W., 2002. The neurophysiology of auditory perception: from single units to evoked potentials. *Audiol. Neurotol.* 7 (2), 71–99.
- Feldman, H., Friston, K.J., 2010. Attention, uncertainty, and free-energy. *Front. Hum. Neurosci.* 4, 215.
- Fiebach, C.J., Gruber, T., Supp, G.G., 2005. Neuronal mechanisms of repetition priming in occipitotemporal cortex: spatiotemporal evidence from functional magnetic resonance imaging and electroencephalography. *J. Neurosci.* 25, 3141–3422.
- Friston, K., 2005. A theory of cortical responses. *Philos. Trans. R. Soc. Lond. Ser. B Biol. Sci.* 360, 815–836.
- Friston, K., 2009. The free-energy principle: a rough guide to the brain? *Trends Cogn. Sci.* 13, 293–301.
- Gagnepain, P., Chételat, G., Landeau, B., Dayan, J., Eustache, F., Lebreton, K., 2008. Spoken word memory traces within the human auditory cortex revealed by repetition priming and functional magnetic resonance imaging. *J. Neurosci.* 28, 5281–5289.
- Giuliano, R.J., Karns, C.M., Neville, H.J., Hillyard, S.A., 2014. Early auditory evoked potential is modulated by selective attention and related to individual differences in visual working memory capacity. *J. Cogn. Neurosci.* 26, 2682–2690.
- Gramfort, A., Luessi, M., Larson, E., Engemann, D.A., Strohmeier, D., Brodbeck, C., Goj, R., Jas, M., Brooks, T., Parkkonen, L., Hämäläinen, M., 2013. MEG and EEG data analysis with MNE-Python. *Front. Neurosci.* 7, 267.
- Grau, C., Fuentesmilla, L.L., Marco-Pallarés, J., 2007. Functional neural dynamics underlying auditory event-related N1 and N1 suppression response. *Neuroimage* 36, 522–531.
- Grunwald, T., Boutros, N.N., Pezer, N., von Oertzen, J., Fernandez, G., Schaller, C., Elger, C.E., 2003. Neuronal substrates of sensory gating within the human brain. *Biol. Psychiatry* 53, 511–519.
- Haenschel, C., Vernon, D.J., Dwivedi, P., Gruzelier, J.H., Baldeweg, T., 2005. Event-related brain potential correlates of human auditory sensory memory-trace formation. *J. Neurosci.* 25 (45), 10494–10501.
- Henson, R., Shallice, T., Dolan, R., 2000. Neuroimaging evidence for dissociable forms of repetition priming. *Science* 287, 1269–1272.
- Hsu, Y.F., Hämäläinen, J.A., Waszak, F., 2013. Temporal expectation and spectral expectation operate in distinct fashion on neuronal populations. *Neuropsychologia* 51 (13), 2548–2555.
- Hsu, Y.F., Hämäläinen, J.A., Waszak, F., 2014a. Repetition suppression comprises both attention-independent and attention-dependent processes. *Neuroimage* 98, 168–175.
- Hsu, Y.F., Hämäläinen, J.A., Waszak, F., 2014b. Both attention and prediction are necessary for adaptive neuronal tuning in sensory processing. *Front. Hum. Neurosci.* 8, 152.
- Hsu, Y.F., Hämäläinen, J.A., Waszak, F., 2016. The auditory N1 suppression rebounds as prediction persists over time. *Neuropsychologia* 84, 198–204.
- Hsu, Y.-F., Hämäläinen, J.A., Waszak, F., 2018. The processing of mispredicted and unpredicted sensory inputs interact differently with attention. *Neuropsychologia* 111, 85–91.
- Hsu, Y.F., Le Bars, S., Hämäläinen, J.A., Waszak, F., 2015. Distinctive representation of mispredicted and unpredicted prediction errors in human electroencephalography. *J. Neurosci.* 35, 14653–14660.
- Hsu, Y.-F., Waszak, F., Hämäläinen, J.A., 2019. Prior precision modulates the minimisation of auditory prediction error. *Front. Hum. Neurosci.* 13, 30.
- Hyvärinen, A., Oja, E., 2000. Independent component analysis: algorithms and applications. *Neural Netw.* 13 (4–5), 411–430.
- Jääskeläinen, I.P., Ahveninen, J., Bonmassar, G., Dale, A.M., Ilmoniemi, R.J., Lavonen, S., Lin, F.H., May, P., Melcher, J., Stufflebeam, S., Tiitinen, H., Belliveau, J.W., 2004. Human posterior auditory cortex gates novel sounds to consciousness. *Proc. Natl. Acad. Sci.* 101 (17), 6809–6814.
- Jacobsen, T., Schröger, E., 2001. Is there pre-attentive memory-based comparison of pitch? *Psychophysiology* 38, 723–727.
- Karhu, J., Herrgård, E., Pääkkönen, A., Luoma, L., Airaksinen, E., Partanen, J., 1997. Dual cerebral processing of elementary auditory input in children. *Neuroreport* 8 (6), 1327–1330.
- Knott, V., Millar, A., Fisher, D., 2009. Sensory gating and source analysis of the auditory P50 in low and high suppressors. *Neuroimage* 44 (3), 992–1000.
- Korzyukov, O., Pflieger, M.E., Wagner, M., Bowyer, S.M., Rosburg, T., Sundaresan, K., Elger, C.E., Boutros, N.N., 2007. Generators of the intracranial P50 response in auditory sensory gating. *Neuroimage* 35 (2), 814–826.
- Lange, K., 2009. Brain correlates of early auditory processing are attenuated by expectations for time and pitch. *Brain Cogn.* 69, 127–137.
- Liegeois-Chauvel, C., Musolino, A., Badier, J.M., Marquis, P., Chauvel, P., 1994. Evoked potentials recorded from the auditory cortex in man: evaluation and topography of the middle latency components. *Electroencephalogr. Clin. Neurophysiol.* 92, 204–214.
- Makela, J.P., Hämäläinen, M., Hari, R., McEvoy, L., 1994. Whole-head mapping of middle-latency auditory evoked magnetic fields. *Electroencephalogr. Clin. Neurophysiol.* 92, 414–421.
- Müller, N.G., Strumpf, H., Scholz, M., Baier, B., Melloni, L., 2013. Repetition suppression versus enhancement: it's quantity that matters. *Cerebr. Cortex* 23, 315–322.
- Nätänen, R., Jacobsen, T., Winkler, I., 2005. Memory-based or afferent processes in mismatch negativity (MMN): a review of the evidence. *Psychophysiology* 42, 25–32.



- Näätänen, R., Picton, T., 1987. The N1 wave of the human electric and magnetic response to sound: a review and an analysis of the component structure. *Psychophysiology* 24, 375–425.
- Pelizzone, M., Hari, R., Makela, J., Huttunen, J., Ahlfors, S., Hämäläinen, M., 1987. Cortical origin of middle-latency auditory evoked responses. *Neurosci. Lett.* 82, 303–307.
- Picton, T.W., Alain, C., Otten, L., Ritter, W., Achim, A., 2000. Mismatch negativity: different water in the same river. *Audiol. Neurotol.* 5, 111–139.
- Ponton, C., Eggermont, J.J., Khosla, D., Kwong, B., Don, M., 2002. Maturation of human central auditory system activity: separating auditory evoked potentials by dipole source modelling. *Clin. Neurophysiol.* 113, 407–420.
- Quiroga-Martinez, D.R., Hansen, N.C., Højlund, A., Pearce, M., Brattico, E., Vuust, P., 2019. Reduced Prediction Error Responses in High- as Compared to Low-Uncertainty Musical Contexts. <https://doi.org/10.1101/422949> bioRxiv. 422949.
- Rao, R.P., Ballard, D.H., 1999. Predictive coding in the visual cortex: a functional interpretation of some extra-classical receptive-field effects. *Nat. Neurosci.* 2, 79–87.
- Recasens, M., Leung, S., Grimm, S., Nowak, R., Escera, C., 2015. Repetition suppression and repetition enhancement underlie auditory memory-trace formation in the human brain: an MEG study. *Neuroimage* 108, 75–86.
- Reite, M., Teale, P., Zimmerman, J., Davis, K., Whalen, J., 1988. Source location of a 50 msec latency auditory evoked field component. *Electroencephalogr. Clin. Neurophysiol.* 70, 490–498.
- SanMiguel, I., Todd, J., Schröger, E., 2013. Sensory suppression effects to self-initiated sounds reflect the attenuation of the unspecific N1 component of the auditory ERP. *Psychophysiology* 50, 334–343.
- Schafer, E.W., Amochaev, A., Russell, M.J., 1981. Knowledge of stimulus timing attenuates human evoked cortical potentials. *Electroencephalogr. Clin. Neurophysiol.* 52, 9–17.
- Schafer, E.W., Marcus, M.M., 1973. Self-stimulation alters human sensory brain responses. *Science* 181, 175–177.
- Schröger, E., Marzecová, A., SanMiguel, I., 2015. Attention and prediction in human audition: a lesson from cognitive psychophysiology. *Eur. J. Neurosci.* 41, 641–664.
- Schröger, E., Wolff, C., 1996. Mismatch response of the human brain to changes in sound location. *Neuroreport* 7 (18), 3005–3008.
- Segaert, K., Weber, K., de Lange, F.P., Petersson, K.M., Hagoort, P., 2013. The suppression of repetition enhancement: a review of fMRI studies. *Neuropsychologia* 51, 59–66.
- Soldan, A., Zarahn, E., Hilton, H.J., Stern, Y., 2008. Global familiarity of visual stimuli affects repetition-related neural plasticity but not repetition priming. *Neuroimage* 39, 515–526.
- Southwell, R., Baumann, A., Gal, C., Barascud, N., Friston, K., Chait, M., 2017. Is predictability salient? A study of attentional capture by auditory patterns. *Philos. Trans. R. Soc. Lond. B Biol. Sci.* 372, 1714, 20160105.
- Subramaniam, K., Faust, M., Beeman, M., Mashal, N., 2012. The repetition paradigm: enhancement of novel metaphors and suppression of conventional metaphors in the left inferior parietal lobe. *Neuropsychologia* 50, 2705–2719.
- Summerfield, C., Trittschuh, E.H., Monti, J.M., Mesulam, M.M., Egner, T., 2008. Neural repetition suppression reflects fulfilled perceptual expectations. *Nat. Neurosci.* 11, 1004–1006.
- Summerfield, C., Wyart, V., Johnen, V.M., de Gardelle, V., 2011. Human scalp electroencephalography reveals that repetition suppression varies with expectation. *Front. Hum. Neurosci.* 5, 67.
- Taulu, S., Simola, J., Kajola, M., 2005. Applications of the signal space separation method. *IEEE Trans. Signal Process.* 53, 3359–3372.
- Timm, J., SanMiguel, I., Saupe, K., Schröger, E., 2013. The N1-suppression effect for self-initiated sounds is independent of attention. *BMC Neurosci.* 14, 2.
- Todorovic, A., van Ede, F., Maris, E., de Lange, F.P., 2011. Prior expectation mediates neural adaptation to repeated sounds in the auditory cortex: an MEG study. *J. Neurosci.* 31, 9118–9123.
- Todorovic, A., de Lange, F.P., 2012. Repetition suppression and expectation suppression are dissociable in time in early auditory evoked fields. *J. Neurosci.* 32, 13389–13395.
- Waldo, M.C., Freedman, R., 1986. Gating of auditory evoked responses in normal college students. *Psychiatry Res.* 19, 233–239.
- Weisser, R., Weisbrod, M., Roehrig, M., Rupp, A., Schroeder, J., Scherg, M., 2001. Is frontal lobe involved in the generation of auditory evoked P50? *Neuroreport* 12, 3303–3307.
- Wiggs, C.L., Martin, A., 1998. Properties and mechanisms of perceptual priming. *Curr Opin Neurobiol.* 8 (2), 227–233.
- Yvert, B., Fischer, C., Bertrand, O., Pernier, J., 2005. Localization of human supratemporal auditory areas from intracerebral auditory evoked potentials using distributed source models. *Neuroimage* 28 (1), 140–153.